Bull. Mater. Sci., Vol. 40, No. 4, August 2017, pp. 783–789
DOI 10.1007/s12034-017-1427-8

Investigation on the bulk growth of α-$LiIO_3$ single crystals and the influence of pH on its structural, morphological and optical characteristics

A SILAMBARASAN[1,*], P RAJESH[1], P RAMASAMY[1], A K KARNAL[2], RAJEEV BHATT[2], INDRANIL BHAUMIK[2] and P K GUPTA[2]

[1]Department of Physics, Research Centre, SSN College of Engineering, Kalavakkam 603110, India
[2]Crystal Growth Laboratory, LMDDD, Raja Ramanna Centre for Advanced Technology, Indore 452013, India
*Author for correspondence (kavianbuarasu@gmail.com)

MS received 29 February 2016; accepted 24 November 2016; published online 26 July 2017

Abstract. α-$LiIO_3$ is an excellent optical material exhibiting strong nonlinear optical, piezoelectric and elasto-optic properties. However, its practical applications are limited by the insufficient reproducibility of the mentioned properties caused by the strong influence of the growth conditions, and, in particular, pH of the solution from which α-$LiIO_3$ crystal is grown. Herein, we investigate to grow bulk size good quality crystals of α-$LiIO_3$ based on the observed problems during its crystallization process. A systematic investigation was carried out to find the effect of pH on solubility, crystal growth, structural, surface and laser damage properties of α-$LiIO_3$ single crystals. The structure and phase of $LiIO_3$ were confirmed by powder X-ray diffractometer analysis. The functional groups of the compound were identified using Fourier transform infrared spectroscopy. Surface defects of the grown crystals were studied by etch patterns. The crystal grown at pH 10 showed 10% optical transmission enhancement in comparison to the crystals grown at pH 2. The indirect optical bandgap of the crystal was reinvestigated using ultraviolet–Visible–near-infrared transmittance spectrum. The laser damage threshold studies of the crystals grown at pH 10 reveal the higher optical radiation stability against 532 nm laser. The second-order nonlinear optical behaviour of α-$LiIO_3$ crystals grown at different pH conditions have been investigated by using Kurtz and Perry powder technique with Nd:YAG laser pulses at the wavelength of 1064 nm.

Keywords. Optical materials; crystal growth; platform technique; X-ray diffraction; surface analysis; frequency doubling.

1. Introduction

For the past five decades, the application of optical materials is intensively devoted to laser communications, laser display, optical storage, bio-photonics, integrated circuits, image processing, marking and precision micro-fabrications, etc. Lithium iodate ($LiIO_3$) is one such excellent optical material exhibiting strong nonlinear optical, piezoelectric and elasto-optic effects, presented by its α-phase polymorph [1–3]. The α-, γ- and β-polymorphs of $LiIO_3$ exist in the solid state belonging to $P6_3$ (hexagonal), $Pna2_1$ (orthorhombic) and $P4_2/n$ (tetragonal) space groups, respectively [4]. α-$LiIO_3$ is a negative uniaxial crystal and the high nonlinear coefficients of d_{31} at 1.06 μm = 4.1 pm V^{-1} is greater than that of KTP [3], which make it very useful optoelectronic and quantum electronic devices [5,6]. Since the iodine atoms (I^{5+}) of α-$LiIO_3$ is more strongly bound to three of its six oxygen ions in the octahedron, this led to 52% density of oxygen atoms in the hexagonal packing of α-$LiIO_3$ [7]. This arrangement of molecules in the crystal attributed to polar C3 symmetry, and it determines the nonlinear properties of the compound [8]. Its wide transparency range from 300 nm to 5 μm is very interesting for applications in the infrared range [3]. In addition, some new applications in the fields of Raman laser, optical data storage have been reported [9–12] and permanent optical waveguides produced by proton implantation in α-$LiIO_3$ crystals were studied [13]. By considering the significant technological application of the material, the growth of α-$LiIO_3$ has been performed by many authors. The influences of pH on the morphology and growth rate of the crystals were investigated in space [14–16]. The fundamental possibility of increasing the crystal growth rate several times with the conservation of crystal quality was demonstrated [17]. The conditions for the growth of hexagonal and a tetragonal form of $LiIO_3$ using the evaporation method were reported [18–20]. As the $LiIO_3$ is quite sensitive to the pH value of mother solution, the influences of pH on electrical properties of α-$LiIO_3$ are studied [21–23]. Though many articles devoted to this problem were published for last 40 years, it is still far from resolved. The flat solubility, pH and temperature of the mother liquor, the formation of two stable phases (α, β) during crystallization, the hygroscopicity of the crystal, etc. are creating a problem in the crystal growth of α-$LiIO_3$. The consequence of such problems is irreproducibility. Also, the influence of pH on structural, surface and laser damage properties of $LiIO_3$ crystal has not been reported. In this context, the present study explains the

effect of pH on crystal growth, structural, surface and linear and nonlinear optical properties of $LiIO_3$. Several contradicting reports on indirect optical bandgap value of α-$LiIO_3$ (varying from 1.7 to 4.4 eV [3,24–26]) suggest reinvestigation.

2. Experimental

2.1 *Materials and solubility*

Lithium carbonate (SRL Chemicals, >99%) and iodic acid (Lobo, >99%) were used for synthesis. The required quantity of lithium carbonate and iodic acid was estimated from the following reaction

$$Li_2CO_3 + 2HIO_3 \rightarrow 2LiIO_3 + H_2O + CO_2$$

This synthesized solution was heated and kept for evaporation to dry and salt was collected. The purity of the synthesized salt was increased by successive recrystallization process and solution was prepared using the deionized water. pH of the mother solution was 2 and it was further increased by the addition of lithium hydroxide. The solubility of the $LiIO_3$ was estimated at pH 2 and pH 10 from 10 to 65°C in the aqueous solvent. The solubility diagram of the $LiIO_3$ is shown in figure 1a. It shows that at pH 10, the solubility is low compared to pH 2 and small negative temperature coefficient of solubility was found. It is comparable with the solubility of $LiIO_3$ measured at pH ~8.5 and it is found to be 80–80.4 g per 100 ml of water in the temperature range of 20–70°C [20].

2.2 *Crystal growth*

Initially, the crystals were grown by the slow evaporation solution technique (SEST). For the growth of crystals, the recrystallized materials were collected and dissolved in aqueous solution and then the saturated solution was filtered and kept in the water bath at 60°C. Once the crystallization condition occurs, the higher solute contents in the saturated solution and flat solubility behaviour of the $LiIO_3$ leads to spurious nucleation. The formation of spurious crystals in the growth vessel is shown in figure 1b and c. During the initial runs of α-$LiIO_3$ crystal growth at pH 2, 4, 5, 6 and 10, we have observed that the crystals grown at pH 10 have higher growth rate than the crystals grown at lower pH conditions and the crystals grown at above the pH 5 have been harvested with good optical quality. This observation matches with the reported results by Chen *et al* [16] that among the α-$LiIO_3$ crystals grown at range of pH from 2.1 to 10.23, the crystals grown at pH 10.23 had relatively higher growth rate. Similarly, Avdienko *et al* [27] reported that the crystals grown at pH 5 have better optical quality than the crystals grown at lower pH. Hence, we choose synthesized salt of $LiIO_3$ at pH 10 in comparison to the synthesized salt at pH 2 for the further studies. α-$LiIO_3$ crystals grown at pH 10 have higher growth rate compared to the crystals grown at pH 2. Moreover, the crystals grown at pH 2 lose transparency and become milky once the crystals are taken out from the mother solution. The α-$LiIO_3$ single crystals grown at pH 2 and 10 by SEST method are shown in figure 2a. The morphology of the crystal as shown in figure 2c was deduced from WinXmorph software. α-$LiIO_3$ crystals grown at pH 10 have higher growth rate compared to the crystals grown at pH 2. In addition, at pH 10, the crystals grown along [001] direction have higher growth rate than the crystals grown along [00$\bar{1}$]. Since α-$LiIO_3$ is a polar crystal, [001] direction possesses a positive charge, and the opposite [00$\bar{1}$] direction possesses negative charge, the dissolution is always more in positive direction than the negative direction when the pH of mother solution is greater than 2.40 [16]. Hence the hydrogen ions play an important role in changing the chemical bonding situations of α-$LiIO_3$.

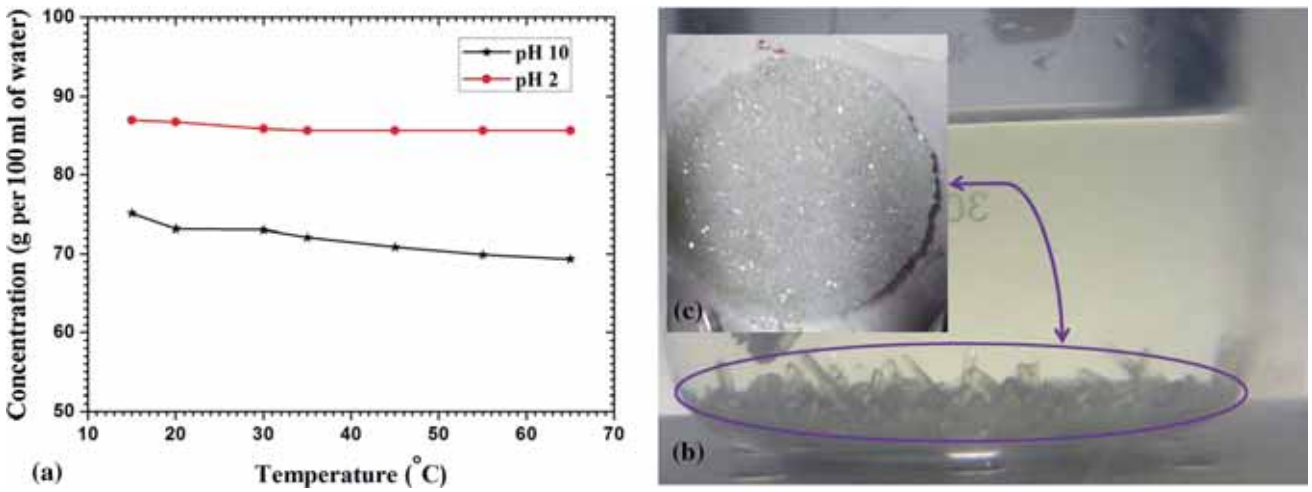

Figure 1. (**a**) Solubility of $LiIO_3$ in aqueous solvent, (**b**) spurious crystals at the bottom of the growth vessel and (**c**) the harvested spurious crystals.

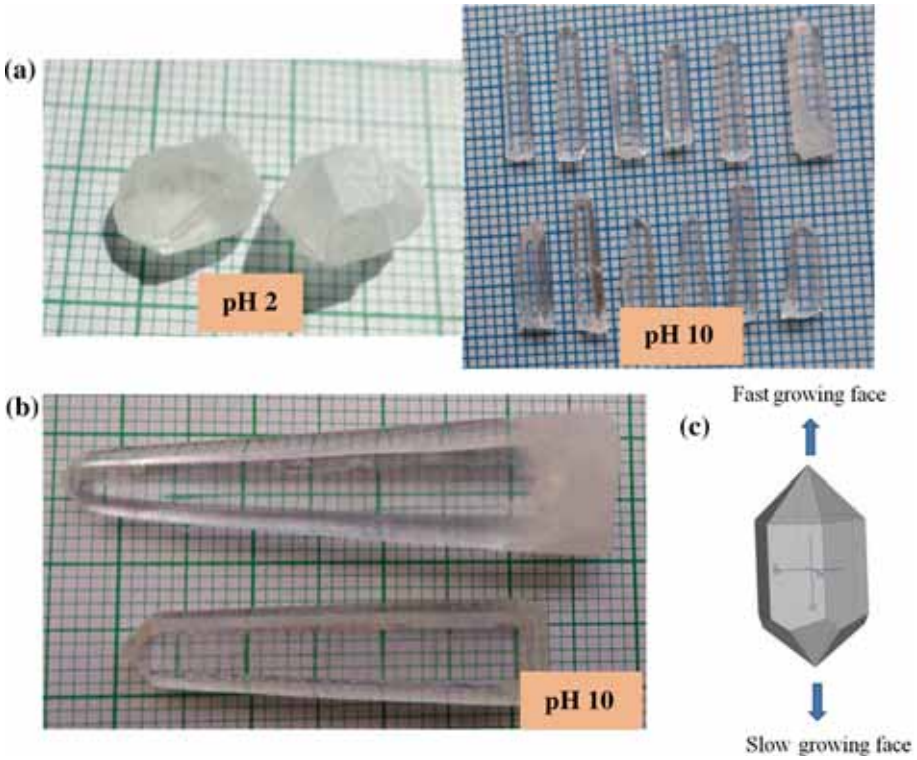

Figure 2. α-$LiIO_3$ crystals grown by (**a**) SEST, (**b**) platform growth techniques and (**c**) morphology of the crystal.

Since α-$LiIO_3$ single crystals grown at pH 10 have visibly better quality, the efforts have been taken to grow bulk size α-$LiIO_3$ crystals by point-seeded platform growth technique. In order to grow the large crystal from the point seed, a good quality seed crystal grown at pH 10 from SEST is chosen to mount in the centre of crystallizer assembly. A homemade acrylic-based seed rotation assembly was used for this purpose. Crystal was mounted in the centre of crystallizer assembly which was attached with controller to rotate in the clockwise direction at a speed of 45 rpm. The uniform rotation of the seed is required so as not to produce stagnant regions or recirculating flows, otherwise inclusions in the crystals will be formed due to inhomogeneous supersaturation in the solution. The rate of temperature raise was maintained at 0.02°C h^{-1}. This very low temperature rise is due to $LiIO_3$ being more soluble (72 g per 100 ml of water at 60°C) than other crystals, thus, more $LiIO_3$ can precipitate at a relatively small degree of supersaturation, and this effect gives spurious nucleation at the bottom of the solution and reduces the growth rate. Also, the dissolution of $LiIO_3$ is trickier because of its very higher solubility. Thus, the growth of $LiIO_3$ is more difficult than that of other materials, and $LiIO_3$ may more easily develop inclusions due to its flat solubility behaviour. In the experiment, we strictly controlled the supersaturation of the solution and finally obtained good quality transparent crystals of size $40 \times 10 \times 10\,mm^3$ in the span of 25 days. The average growth rate of the crystal was 1.5 mm per day. The grown crystals are shown in figure 2b, and reveal no visible macroscopic defects.

2.3 *Instrumentation*

The powder X-ray diffractometer (XRD) spectrum of the salt synthesized at pH 2 and 10 was recorded in the scanning step time of $10\,deg\,s^{-1}$ over a 2θ range of 10 to 80° by using a Philips XPert Pro X-Ray diffractometer with Cu K α radiation of wavelength 1.5418 Å. The Fourier transform infrared (FTIR) analysis is important to understand the various functional groups in the structure of a compound. The spectrum was recorded using ALPHA FTIR spectroscopy in the wavelength range 500–4000 cm^{-1} by KBr pellet technique. The as-grown crystals are immediately examined after etching, and its microstructures were analysed by using OLYMPUS U-TV0.5XC-3 optical microscope in the reflection mode. The optical transmittance was recorded from ultraviolet (UV) to near-infrared (NIR) in the wavelength range of 200–1100 nm using Perkin Elmer UV–Vis–NIR spectrophotometer at room temperature. The surface polished $LiIO_3$ samples of 2-mm thickness without any coating were used for optical measurements. A Q-switched Nd:YAG laser delivering ns pulses of a wavelength at 532 nm (7 ns, 10 Hz) was used for laser damage studies (LDT). (010) face of $LiIO_3$ samples identical in thickness and surface finish (polishing) were kept 1 cm above focus point of the laser for the measurements where the spot size is

220 μm, and the energy of the laser was measured using an energy power meter (EPM 2000) attenuated using appropriate neutral density filters. The nanosecond laser was focused on to the target crystal by a plano-convex lens of 100 mm focal length. The sample was kept 1 cm above focus point of the laser for the measurements. In order to measure SHG output, the powdered samples of α-$LiIO_3$ crystals grown at pH 2 and 10 were irradiated with a pulsed infrared beam (5 ns, 10 Hz) produced by a Q-switched Nd:YAG laser at wavelength of 1064 nm and the energy of the laser pulse was around 1.6 mJ per pulse. The monochromator was set at 532 nm to eliminate fundamental frequency. When the laser hit on the sample, the green emission was detected using an energy metre. The signals were captured with an Agilent infinium digital storage oscilloscope interfaced to a computer.

3. Results and discussion

3.1 *Structural analysis*

Figure 3 shows powder XRD patterns of $LiIO_3$ salt synthesized at pH 2 and 10. Powder XRD patterns of α-$LiIO_3$ are observed for both pH; in addition to this, several peaks of β-$LiIO_3$ have also been observed for the salt synthesized at pH 2. It suggests that pH of the solution influences the structure and phase of $LiIO_3$. It confirms the formation of two stable phases of α-$LiIO_3$, and it is one of the major problems in growing bulk α-$LiIO_3$ crystals. Umezava and Tatuoka [20] have reported that the solubility of β-$LiIO_3$ is 1–2% higher than that of α-$LiIO_3$ when the pH of the solution is in between 8.3 and 8.7. The formation of β-$LiIO_3$ crystals in addition to α-$LiIO_3$ crystals in the saturated solution of pH 2 is the reason to have higher solubility of the $LiIO_3$ salt synthesized at pH 2. The introduction of pH 10 in mother liquor of $LiIO_3$ leads to the growth of α-phase of $LiIO_3$ crystals alone. Also, the crystals grown at pH 10 have very sharp peaks with high intensity; it is because of the perfect crystallization of the material.

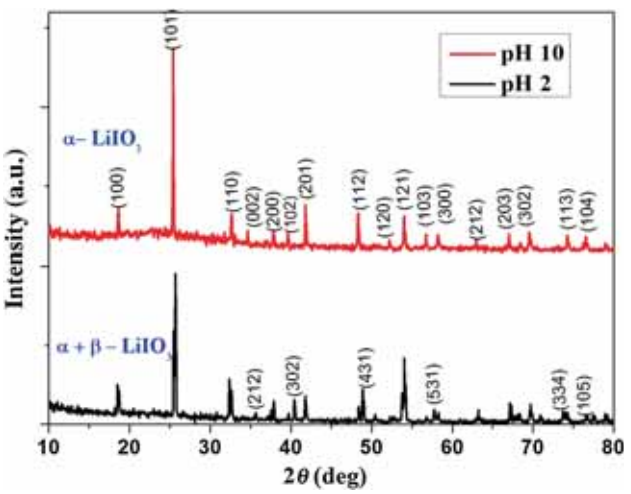

Figure 3. Powder X-ray diffraction pattern of $LiIO_3$ salt synthesized at pH 2 and pH 10.

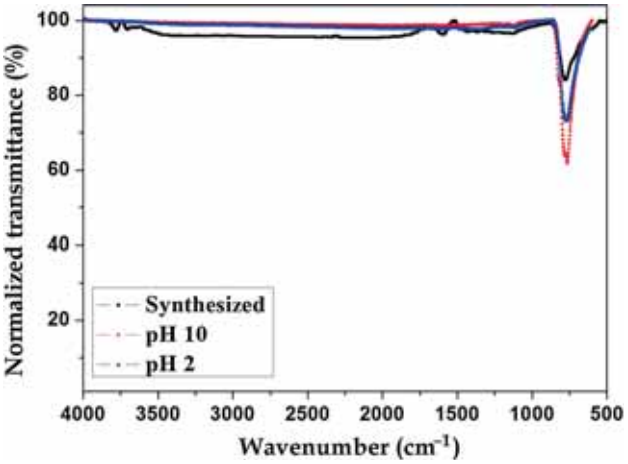

Figure 4. FTIR spectrum of synthesised $LiIO_3$ and the crystals grown at pH 2 and pH 10 of α-$LiIO_3$.

In order to confirm α- and β-phase of $LiIO_3$, the spectrum was indexed using JCPDS software and it is perfectly matching with JCPDS card nos 88-1745 and 85-0507, respectively. The α-phase of the synthesized salt belongs to hexagonal system, space group is P6, and the lattice parameters are $a = 5.462$ Å, $c = 5.139$ Å, and the β-phase of the synthesized salt belongs to tetragonal system, space group is $P4_2/m$, and the lattice parameters are $a = 9.660$ Å, $c = 6.210$ Å.

The FTIR spectrum of α-$LiIO_3$ crystals grown at pH 2, pH 10 and synthesized materials are shown in figure 4. The strong peak occurring at 784 cm^{-1} as shown in the figure is due to I–O stretching vibration in the grown $LiIO_3$ crystals [28]. Also, it is interesting to note that the absorption corresponding to the I–O stretching bond at 784 cm^{-1} is the strongest with lowest FWHM for the crystal grown at pH 10. This signifies that the crystal quality is better for the crystal grown in pH 10 in comparison to that grown in pH 2. For the synthesized $LiIO_3$ sample, two additional peaks observed at 3600 and 1600 cm^{-1} indicate the presence of stretching vibration of O–H and the CO_3^{2-} group, respectively, characterizing the small content of HIO_3 and Li_2CO_3 in the synthesized material.

3.2 *Morphological analysis*

In utilizing single crystals for various applications, it is essential to grow single crystals with less dislocation density. Etching a crystal for short duration yields etch figures (frequently pits), dissolution layers on its surfaces and also it clearly indicates the crystal imperfections and defects. According to the Cabrera's theory and Monte Carlo simulation of crystal growth, etchants like water and methanol could produce visible etched feature easily within a short time [29,30]. In the present work, etching studies were carried out using water as etchant on the (010) surface (prismatic face) of α-$LiIO_3$ at room temperature. The crystal was dipped in water etchant and the etched surface was smoothly wiped with a dry tissue paper. Figure 5a, c and e represents the

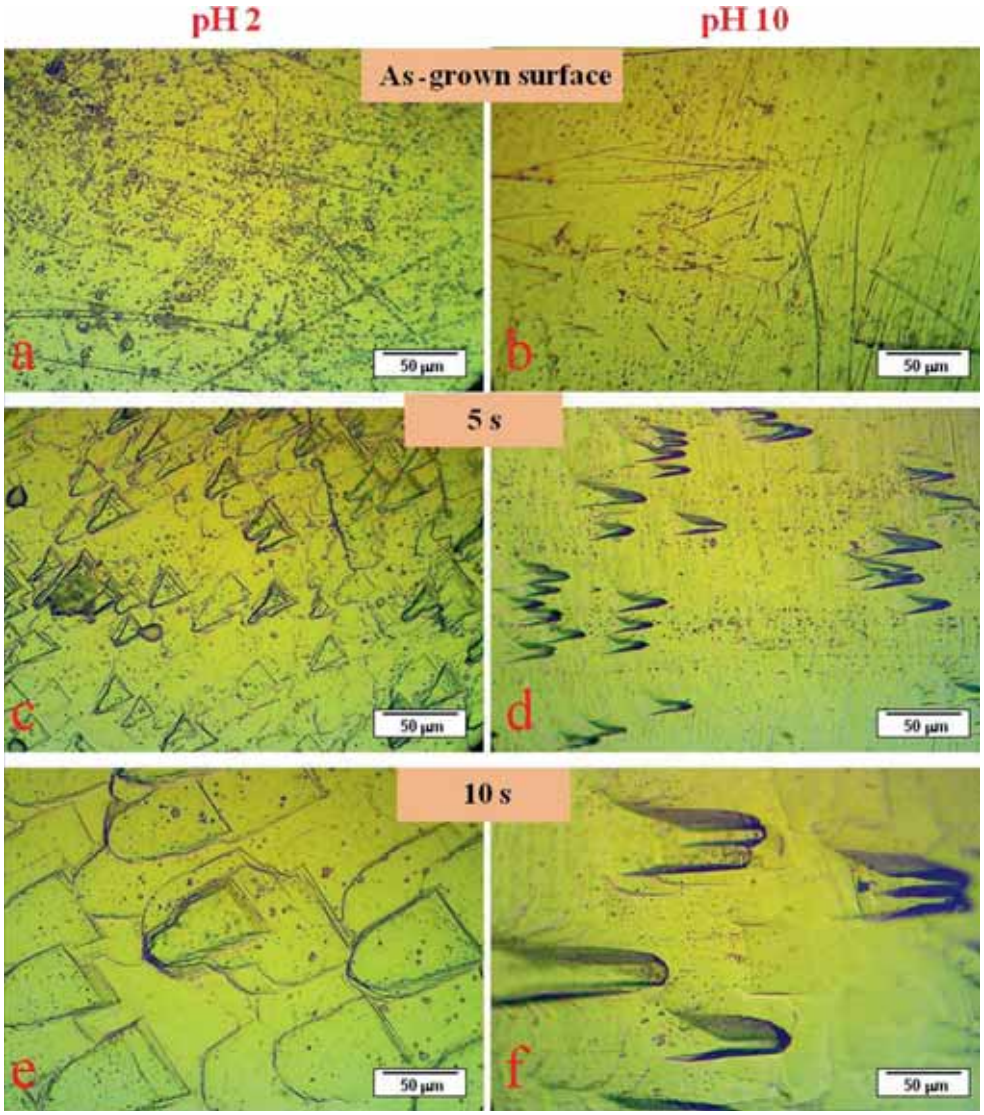

Figure 5. Surface etch pattern of as-grown α-$LiIO_3$ for the different etching time.

microscopic image before and after etching of the as-grown crystal at pH 2, whereas figure 5b, d and f represents the microscopic image before and after etching of the as-grown crystal at pH 10. The micrograph of α-$LiIO_3$ crystal grown at pH 2 shows that the surface of the whole crystal appears rough with isolated islands and minute crystallites; it may be due to moisture absorption on the crystal surface. It was observed that the morphology of the etch pits strongly depends on the nature of etchants and structure of the compound. The hexagon pits parallel to the [001] directions are observed for the different etching time. These pits are nucleated at the sites of the emergence of dislocations intersecting cleavage surface. Etch pits of similar size are obtained along [001] direction of the crystals grown at pH 2 and 10 after etching for 5 s, and are shown in figure 5c and d. An increase in etch time (10 s) resulted in deeper and bigger etch-pits without changing its shape, as shown in figure 5e and f, which proves that these etch pits are imprints of dislocations. This gradual formation of etch pits occurred due to the pits corresponding to dislocations and those of structural defects. It was observed the pits on the (001) face of α-$Li1O_3$ single crystals grown on a pyramidal seed that along with rhombic etch pits, others in the form of hexagon etch pit [31]. However, in the present study, the pits with a symmetrical shape should result from the internal structural symmetries of the crystal. The calculated etch pit density (EPD) for the 5 s of etching time of the crystals grown at pH 2 and 10 are 4.34×10^5 and 3.43×10^5 cm^{-2}, respectively. The difference between the EPD can be attributed to the difference in growth condition, which influences the crystalline perfection. The decrease in EPD is associated with more systematic packing of the atoms during growth, which indicates that the crystals grown at pH 10 in the present study are of good quality.

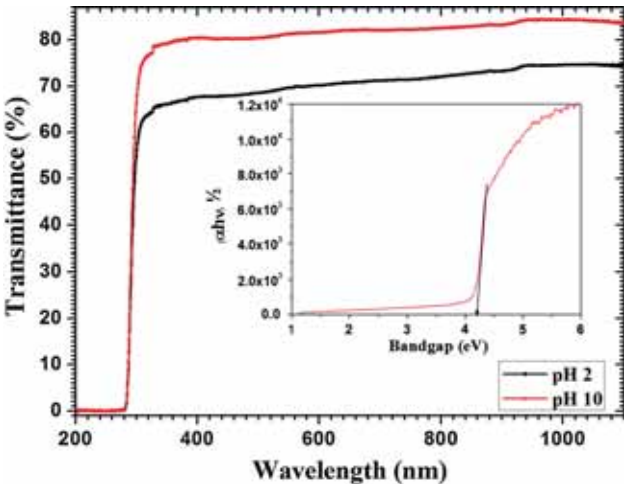

Figure 6. UV–Vis–NIR transmittance spectrum and corresponding Tauc plot of α-$LiIO_3$.

3.3 *Optical characteristics*

Good transparency of the crystal is an essential requirement for many optical applications. The optical transmittance spectra of the crystals grown at pH 2 and 10 of $LiIO_3$ were recorded at room temperature, in which characteristic absorption edge of α-$LiIO_3$ crystal occurred at 284 nm as shown in figure 6. It is observed that both the crystals have wide transparency in the region between 315 and 1100 nm. The figure clearly shows that the grown crystals at pH 2 have 70% transmittance, and the grown crystals at pH 10 have a transmittance of 80% in the visible region. Substantially, 10% higher transmission was observed for the crystals grown at pH 10 compared with the crystals grown at pH 2. The more systematic arrangement of atoms in the crystals grown at pH 10 as evidenced by the etch patterns is attributed to the absence of interstitial and vacancy sites, and it is leading to less absorption and enhanced optical transmittance of the crystal. There are contradicting reports regarding the bandgap (1.7 to 4.4 eV [3,24–26]) of this material. Since the magnitude of the bandgap of solid determines the frequency or wavelength of the light, which will be adsorbed, such a value is very useful for the optoelectronic applications. Hence in the present study, the bandgap of the $LiIO_3$ was determined from the measured transmittance spectrum based on its optically induced transition. As the absorption coefficient is dependent on photon energy, the measured transmittance (T) was used to calculate the absorption coefficient (α), and it was analysed in the absorption regions so as to obtain the detailed information about the band structure and type of transition of the compound. The following equation was used to calculate absorption coefficient (α),

$$\alpha = \frac{2.303 \times \log(1/T)}{t},$$

where T is the transmittance and t the thickness of the sample. The similar absorption coefficient was observed in different parts of the grown crystal. As $LiIO_3$ is an indirect bandgap material, the optical bandgap (E_g) has been estimated from the optical absorption coefficient (α) near the absorption edge for the indirect transition using the following Tauc relation [32]

$$(\alpha h\nu)^{1/2} = A\left(E_g - h\nu\right),$$

where A is a constant, E_g the optical bandgap, h the Planck's constant and ν the frequency of incident photons. The optical bandgap was evaluated by plotting $(\alpha h\nu)^{1/2}$ *vs.* $h\nu$ as shown in the inset of figure 6. The resulting plot has a distinct linear regime, which denotes the onset of absorption. Thus, extrapolating this linear region of absorption edge $(\alpha h\nu)^{1/2}$ straight line in the photon energy axis yields the energy of the optical bandgap of the crystal. From the figure, the optical bandgap value of α-$LiIO_3$ single crystal is obtained to be 4.21 eV. Our results are in close agreement with the result reported by Kang *et al* [24].

Table 1. Surface laser damage threshold values of α-$LiIO_3$ crystals grown at pH 2 and pH 10.

pH value	Laser energy (mJ)	Period (s)	Observation
2	12	20	No damage
	15	15	Small spot
	20	5–6	Big spot with crack
10	12, 15	20	No damage
	20	20	Small spot
	25	8–9	Big spot with crack

Investigation of crystal stability against intense nanosecond/picosecond laser pulses is one of the most important prerequisites for applications in optoelectronic devices. Since the tiny scratches or a little contamination on the surface of the sample can substantially lower the surface damage threshold, the $LiIO_3$ crystal sample was well polished using alumina powder and ethylene glycol to avoid defects, impurities and imperfections on the surface. (010) face of α-$LiIO_3$ crystals grown at pH 2 and 10 were used to measure the laser damage measurements. The detailed LDT profile of the grown α-$LiIO_3$ crystals is given in table 1. It was observed that the crystals grown at pH 2 could withstand up to ~12 mJ and no damage was noticed even after 20 s of exposure. For the same experimental setup, the crystals grown at pH 10 could withstand up to ~15 mJ without any damages. Care was taken to select a fresh region after each shot to avoid cumulative effects resulting from multiple exposures. When the energy of the laser was increased beyond 20 mJ, a small spot appeared on the surface of the crystals grown at pH 10. It is observed that the crystal grown at pH 2 has lower laser stability than the crystal grown at pH 10. Rough and few isolated islands on the surface of the crystal grown at pH 2 may be the reason to have lower laser stability. Nishida *et al* [33] observed similar result for KDP samples, in which the organic impurities seemed to play the main role in causing bulk laser damage to the compound.

In order to measure SHG output of α-$LiIO_3$ relative to KDP, Kurtz and Perry powder technique was used. The conversion efficiency is measured in terms of peak-to-peak voltage and compared with KDP as a reference. The SHG intensities of $LiIO_3$ grown at pH 2, 10 and KDP are 0.52, 0.56 and 0.06 mV, respectively. Hence about 10 times higher SHG signal of α-$LiIO_3$ in comparison to KDP proves it to be a potential candidate for frequency doubling applications**.** The higher SHG signal of α-$LiIO_3$ is because of the alignment of the polarizations of the iodate groups in the *b*-axis, whereas the contributions of the Li-O octahedra are expected to be very small since their distortions are very small [34]. This value is comparable with the measured value of non-linear optical coefficient using Maker fringes technique with respect to KDP: whereas $d_{31}(LiIO_3)/d_{35}$ (KDP) is 12 [35].

4. Conclusions

The two stable phases of $LiIO_3$ at room temperature and flat soluble nature are the two major problems in growing α-$LiIO_3$ crystals. Influence of pH on the solubility of α-$LiIO_3$ was studied, and the single crystals were grown from water solvent at pH 2 and 10 by solution growth technique. The reason for the higher solubility of the crystals grown at pH 2 is because of the formation of β-phase in addition to α-phase of $LiIO_3$. The introduction of alkaline pH (pH 10) in mother liquor of $LiIO_3$ leads to the growth of α-phase of $LiIO_3$ crystals alone. The surface dislocations of grown α-$LiIO_3$ crystals with respect to pH have been examined by etch patterns. The optical transmittance, surface micrograph pattern and laser damage threshold studies of α-$LiIO_3$ reveals that the crystals grown at pH 10 have better quality. It implies that hydrogen ion played a major role in growth rate and crystal quality of the $LiIO_3$ crystals. The recorded UV–Vis–NIR absorbance spectrum was used to reinvestigate the indirect optical bandgap value of α-$LiIO_3$ and it was found to be 4.21 eV. The second harmonic conversion efficiency of α-$LiIO_3$ crystals grown at pH 10 is estimated by Kurtz and Perry powder technique and is comparable with the measured values by Maker fringe technique. We believe that this present investigation has great implications for the development of bulk size α-$LiIO_3$ crystals for still more efficient optoelectronic applications.

Acknowledgement

We gratefully acknowledge DAE-BRNS for the financial support (Ref: No. 2012/34/52/BRNS/2037).

References

[1] Nash F R, Bergman J G, Boyd G D and Turner E H 1969 *J. Appl. Phys.* **40** 5201
[2] Haussuhl S 1968 *Phys. Stat. Sol. (b)* **29** K159
[3] Gang Y, Yu C, Xin-You A, Zhong-Qian J, Lin-Hong C, Wei-Dong W *et al* 2013 *Chin. Phys. Lett.* **30** 67101
[4] Echardt R C, Masuda H, Fan Y X and Byer R L 1990 *J. Quant. Electron.* **26** 922
[5] Choy M M and Byer R L 1976 *Phys. Rev. B* **14** 1693
[6] Haussuhl S 1970 *Acoustica* **23** 165
[7] Avdienko K I, Bogdanov S V, Arkhipov S M, Kidyarov B I, Lebedev V V, Nevsky Y E, Trunov V I, Shelaput D V and Shklovskaya R M 1980 *Lithium iodate: growth, properties and application* (Novosibirsk: Nauka) p 144
[8] Yelisseyev A P, Isaenko L I and Starikova M K 2012 *J. Opt. Soc. Am. B* **29** 6
[9] Liu F Q, He J L, Sun S Q, Xu J L, Zhang B T, Yang H W *et al* 2011 *Laser Phys. Lett.* **8** 579
[10] Jingjun Xu, Kabelka H, Rupp R A, Laeri F and Vieze U 1998 *Phys. Rev. B* **57** 9581
[11] Moreira R L, Bourson P and Rosso C 1995 *Radiat. Eff. Defects Solids* **137** 319
[12] Qian Sun, Rupp R A, Fally M, Vietze U and Laeri F 2001 *Opt. Commun.* **189** 151
[13] Rosso C, Moretti P, Galez C, Mugnier J, Barbier D and Bouillot J 1997 *Opt. Mater.* **8** 237
[14] Chen W C, Li C R and Liu D D 2003 *J. Cryst. Growth* **254** 169
[15] Chen W C, Liu D and Dang J 2007 *J. Jpn. Soc. Microgravity Appl.* **24** 15
[16] Chen W C, Ma W Y, Liu D D and Xie A Y 1987 *J. Cryst. Growth* **84** 303
[17] Rubakha V I and Puchkov A V 2014 *Crystallogr. Rep.* **59** 768
[18] Robertson D S and Roslington J M 1971 *J. Phys. D: Appl. Phys.* **4** 1582
[19] Unezawa T, Ninomiya Y and Tatuoka S 1970 *J. Appl. Cryst.* **3** 417
[20] Umezava T and Tatuoka S 1972 *Jpn. J. Appl. Phys.* **11** 906
[21] Jacobsohn L G, Lunkenheimer P, Laeri F, Vietze U and Loidl A 1996 *Phys. Stat. Sol. B* **198** 871
[22] Dongfeng Xue and Siyuan Zhang 1998 *J. Solid State Chem.* **135** 121
[23] Arend H, Remoissenet M and Staehlin W 1972 *Mat. Res. Bull.* **7** 869
[24] Kang L, Ramo D M, Lin Z, Bristowe P, Qin J and Chen C 2013 *J. Mater. Chem. C* **1** 7363
[25] Jaffer M A and Abu El-Fadl A 1999 *J. Phy. Chem. Solids* **60** 1633
[26] Timokhin V M 2014 *J. Nano-Electron Phys.* **6** 03048
[27] Avdienko K I, Kidyarov B and Sheloput D V 1977 *J. Cryst. Growth* **42** 228
[28] Anayan E S, Balasanyan R N, Vartanyan E S and Chirkinyan S S 1984 *Sov. J. Quant. Electron* **14** 1115
[29] Sangwal K 1987 *Etching of crystals theory, experiment and application* (The Netherlands: Elsevier Science Publisher B.V.)
[30] Human W J, Vander Eerden J P, Jetten L A and Odekerken J G 1981 *J. Cryst. Growth* **51** 589
[31] Muradyan G G, Nalbandyan A G and Sharkhatunyan R O 1981 *J. Cryst. Growth* **52** 936
[32] Bhatt R, Indranil Bhaumik, Ganesamoorthy S, Karnal A K, Swami M K, Patel H S *et al* 2012 *Phys. Status Solidi (A)* **209** 176
[33] Nishida Y, Yokotani T, Sasaki T, Yoshida K, Yamanaka T and Yamanaka C 1988 *Appl. Phys. Lett.* **52** 420
[34] Kong F, Sun C, Yang B and Mao J G 2012 *Struct. Bond* **144** 43
[35] Jerphagnon J 1970 *Appl. Phys. Lett.* **16** 298